4ICEGE
Thessaloniki-GREECE 2007

4th International Conference on
Earthquake Geotechnical Engineering
June 25-28, 2007
Paper No. 1763

SOIL STABILITY UNDER EARTHQUAKES: A SENSITIVITY ANALYSIS

Carolina SIGARÁN-LORÍA [1], Amir M. KAYNIA[2], and Robert HACK[3]

ABSTRACT

The slope stability behaviour of cohesive and cohesionless soil slopes was evaluated under earthquakes with different frequencies and amplitudes (0.01 to 1.0 g). The study focused on the computation of slope instability thresholds at different slope heights (5, 10 and 15 m) and inclinations. This parametric analysis was performed with a nonlinear finite element method (*FEM*) in plane strain using the Mohr Coulomb constitutive model and accounting for stiffness and strength increase with depth.

The steepest slope for each soil type was defined as the slope at its marginal stability with a safety factor under static conditions between 1.01-1.06. All the acceleration histories were sinusoidal functions at frequencies of 1, 2 and 4 Hz. The amplitude of these accelerations was gradually increased until the point they initiated instabilities in the slopes. These accelerations were denoted by critical peak accelerations (*PGAc*). This study demonstrates that lower peak accelerations (*PGA*) are needed to trigger instabilities at steeper slopes. Also, the highest frequency used in this parametric study (4 Hz) has higher *PGAc*, and in most cases the lowest frequency (1 Hz), which is close to the natural frequencies of the site (0.6 to 1 Hz) experience the lowest *PGAc*. The strength of the materials also governs the sliding thresholds, being higher for the stronger ones.

Keywords: Earthquake, landslide, slope instability, numerical modelling, finite elements, parametric analysis

INTRODUCTION

Strong earthquakes can potentially trigger landslides that can be catastrophic for human lives and the infrastructure. Around 20% of the registered landslides are triggered by earthquakes (Wen et al., 2004). China is the country with most casualties associated to slides (Leroueil, 2001) and many seismic active countries around the world have records of different sizes of slope failures that have left tremendous damages and casualties, some examples per region are:

- Pacific coastline of Central and Southern America. Bommer & Rodríguez (2002) present an extensive list of earthquakes that have triggered slides in Central America, common phenomena associated to the presence of weak volcanic rock masses and deep lateritic soils. The majority

[1] PhD Student, ESA Department, International Institute for Geo-Information Science and Earth Observation, and Faculty of Civil Engineering and Geosciences, Technical University of Delft, The Netherlands, Email: sigaran@itc.nl
[2] Discipline Manager, Earthquake Engineering, Norwegian Geotechnical Institute, Norway, Email: amir.m.kaynia@ngi.no
[3] Associate Professor, ESA Department, International Institute for Geo-Information Science and Earth Observation, Email: hack@itc.nl

of these seismic events are registered to have been shallow (<10 km hypocentral depth). Based on the spatial distribution, it is suggested that the slope instabilities correspond to the exceedance of a particular ground-motion threshold (Bommer & Rodríguez, 2002; Keefer, 1984). In Colombia, Ecuador, Peru, and Chile strong earthquakes have triggered many slides in volcanic settings (Tibaldi et al., 1995; Rodríguez et al., 1999; Bommer & Rodríguez, 2002; and Bird & Bommer, 2004).

- Japan. Seismically triggered landslides in volcanic weathered materials are common (Tanaka, 1985; Fukuoka et al., 2004; Sassa et al., 2004; Trandafir & Sassa, 2005; and Uzuoka, 2005).
- Pacific coastline of the United States and Canada. Keefer (1984, 1998, 2000), and Ashford & Sitar (2002) mention cases on steep slopes (marine terraces) in weakly cemented soils. Zeghal et al. (1999) report an important slope failure triggered by liquefaction during the San Fernando earthquake of 1971.
- Central Asia (China, Taiwan, Kyrgyzstan, Pakhistan, Afghanistan, India, Nepal). Giant catastrophic slides (>10^7 m^3) have been triggered in China and thousands of slides have been reported in Taiwan from a single event (Chi-Chi earthquake in 1999) in different geological environments (e.g. loess, metamorphic and sedimentary discontinuous rock masses) (Leroueil, 2001; Havenith et al., 2002, 2003; Wen et al., 2004; Khazai & Sitar, 2003; Chang et al., 2005; and Sepúlveda et al., 2005).
- Mediterranean region. In Greece, Turkey and Italy, several landslides have been triggered by strong earthquakes in different geological settings as reported by Papadopoulos & Plessa (2000), Cotecchia and Melidoro (1974), Cotecchia et al. (1986), Esposito et al. (2000), Prestininzi & Romeo (2000), Nicoletti & Parise (2002), Porfido et al. (2002), Wright & Rathje (2003).

Not all earthquake-induced slides have occurred in areas with records of landslides or at locations with instabilities under static conditions (Keefer, 1984). The most important variables that affect the slope stability are: (a) geomechanical parameters of the ground, (b) geometry of the slope, and (c) characteristics of the dynamic load.

Geomaterials can modify the way seismic waves propagate and generate either amplification, attenuation or tensional effects in the ground influencing the deformation and eventual ground failure (Kramer & Stewart, 2004). Damping, stiffness and shear strength of the ground govern the site effects. The reduction in the shear strength is one of the major causes of most of the slides induced by earthquakes (Wright & Rathje, 2003). Groundwater when present may play a definite role as well. In Italy, Wasowski et al. (2002) observed that during the Irpinia earthquake (1980) the change in the groundwater condition (seismically induced pore-water pressure rise) was a major controlling parameter in the spatial landslides distribution. The energy content of the earthquake close to the natural period of the site will be more amplified and will lead to increased failure potential. The extent of landslides is related to the magnitude and nature of the event, and the sizes of failures are dependent on the relation between the slope aspect and the ground shaking (Li, 1978 in Wen et al., 2004). The spatial distribution of landslides decreases exponentially from the fault rupture area (Porfido et al., 2002).

Landslides triggered by earthquakes can be classified in three main groups according to their fragmentation and placement mechanisms (Varnes, 1978): (1) disrupted slides and falls, which occur fast and at high inclinations (>35°) in discontinuous rock masses or weakly cemented materials; (2) coherent slides, either in rock or soil with deep slip weakened surfaces or with a relatively broad distributed shear zone, reported for inclinations >15°; and (3) lateral spreads and flow slides, associated to liquefaction in granular materials; if residual strengths are lower than static shear stresses, flow slides can develop at very low inclinations. According to Keefer (1984) the first two are the most common.

Traditionally, the dynamic slope stability has been estimated from pseudo-static approaches, using linear or equivalent linear methods, or displacement based methods (e.g. Newmark). The sliding block procedure is conservative when the predominant frequency of the input motion exceeds the natural frequency of the mass (Wartman et al., 2003). The behaviour of soils in connection with slope response has been characterized extensively by experimental methods; examples include the ring shear test for undrained cohesionless soils (e.g. Zergoun & Vaid, 1994; Sassa et al., 2004; Trandafir & Sassa, 2005), dynamic centrifuge simulations (e.g. Popescu & Prevost, 1993; Taboada-Urtuzuastegui et al., 2002; Kagawa et al., 2004; Ng et al., 2004; Lu, 2006; Azizian & Popescu, 2006; Nabeshimal et al., 2006), H/V and standard spectral ratios to assess site effects (e.g. Havenith et al., 2002). Recently, Kokusho & Ishizawa (2006) proposed an energy balance approach for the model of a rigid block lying on an inclined plane. The method was developed using measurements in a sliding slope of dry sand on a shaking table and evaluation of the earthquake energy needed to induce slip.

Stress-deformation analyses with numerical tools are becoming more common because they can provide insight of the nonlinear behaviour of the material. Numerical methods (finite differences, *FD* and *FE* mainly) have been applied to case studies. Examples on subaerial slopes are Havenith et al. (2002, 2003), Bourdeau et al. (2004), Crosta et al. (2005), Chugh & Stark (2006), who present two dimensional models with *FD* of cases from Kyrgyzstan, El Salvador, California, using different constitutive models (e.g. Mohr Coulomb, softening). Bourdeau et al. (2004) noticed that two-dimensional numerical models give smaller failed areas than pseudostatic and static slope stability analyses. Chugh & Stark (2006) found similar displacements in their results as obtained with the Newmark displacement-based method. Loukidis et al. (2003) compared *FE* in a linear approach with pseudostatic evaluations and obtained similar results for the selected cases. Azizian & Popescu (2006) used two-dimensional (*2D*) and three-dimensional (*3D*) *FE* models and defined ranges within which non-linear *2D FE* analyses can be applicable for earthquake slope stability assessments in the context of submarine slopes. In their assessed cases, *2D* analyses showed sufficient accuracy for slopes smaller than 20°. For these cases, they found that resultant displacements, strains and stresses are similar in shape for *2D* and *3D* models, but *2D* analyses are more conservative, and have shown to be closer to centrifuge experimental observations. These are consistent with the observations of Ghosh & Madabhushi (2003). The latter authors concluded from their non-linear *FE* evaluations that responses with simple input motions are easier to understand than to motions with wide frequency ranges, such as real earthquakes, although the energy content would differ and result in a biased response. Numerical methods have been calibrated against experimental ones (e.g. Havenith et al., 2002; Ghosh & Madabhushi, 2003; Azizian & Popescu, 2006; Lu, 2006). Lu (2006) developed a *3D* parallel non-linear coupled *FE* for earthquake ground response and liquefaction based on a serial code. This enables running very large models within reasonable time. The build-up of the models is complicated but user-friendly interfaces are planned to be developed.

This paper presents a parametric study of acceleration thresholds for earthquake induced slope instability for generic cohesive and cohesionless soils by incorporating geotechnical, topographical and input seismic signal features. The analyses are carried out under ideal and simplified conditions of the slope and input acceleration in order to highlight the impact of the various parameters and make observations on the possible modes of failure. It should be emphasized that the objective is not to make general conclusions or establish guidelines for design. The parameters studied here are the slope height and inclination, geotechnical characteristics of the soil, and the frequency of the earthquake excitation.

ADDRESSED PROBLEM & FORMULATION

Two-dimensional plane strain step-like slopes (Figure 1) were assessed with *FEM*. The critical acceleration (*PGAc*) at bedrock of the slopes were determined for variable slope heights (*H*), slope inclinations (*i*) and frequencies (*f*), using sinusoidal-type acceleration time histories (Figure 2) and a constant depth below the base of the slope. Although monochromatic input motion may lead to

biased results, it was used for simplicity and to isolate the effect of the excitation's frequency and amplification of the waves through the slope.

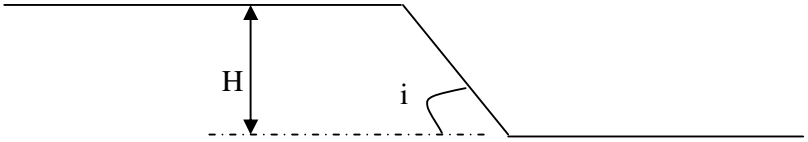

Figure 1. Slopes geometry and geometrical features

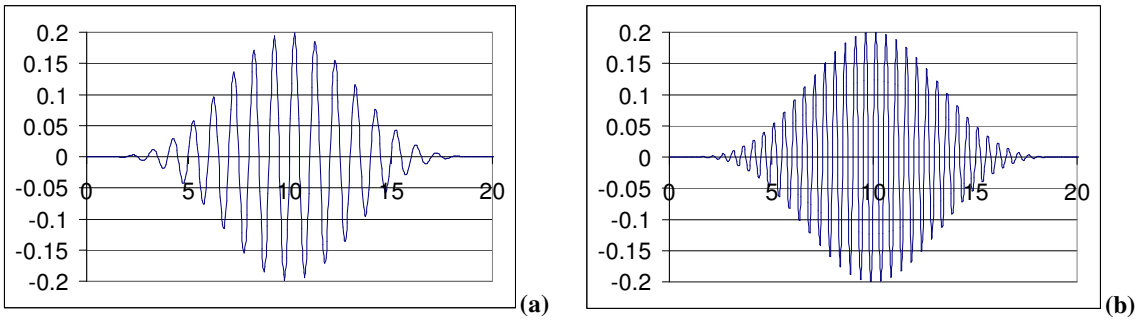

Figure 2. Examples of acceleration time histories used: (a) *PGA*=0.2 g, *f*=1 Hz; (b) *PGA*=0.2 g, *f*=2 Hz

Two types of materials were assessed: sand and clay, both under dry conditions for simplicity. Furthermore, two types of clay with different strengths, for a total of three types of soil, one sand and two clays. The clay with lower strength was denoted as "clay 1", and the one with higher strength was denoted as "clay 2".

Model features

All the models had the same dimensions of approximately 400 m width and 50 m depth below the slope base. The side boundaries were placed at large enough distances of the slope to avoid possible reflections. The mesh was made of 15-noded triangular elements and was fine enough to insure appropriate wave propagation in accordance with the wavelength and shear wave velocities. The models were further refined towards the ground surface.

Slope geometries

The slope heights and inclinations used in this study are listed in Table 1. In each case, the largest slope angle was computed as the angle corresponding to the marginal static stability of the slope, that is, with a safety factor (*FS*) between 1.01 and 1.06 (Table 2 and Figure 3).

Table 1. Heights and inclinations of the assessed slopes

Slope height (*H*, m)	Slope inclination (*i*, °)		
	Sand model	Clay 1 model	Clay 2 model
5	15°, 20°, 25°, 30°, 35°	5°, 10°, 20°, 30°	30°, 40°
10	10°, 15°, 20°, 25°, 30°, 32°	5°, 10°, 15°, 20°	5°, 10°, 20°, 25°
15	10°, 15°, 20°, 25°, 30°	17, 15°, 10°, 5°	10°, 15°, 22°

In the static calculations the side and bottom boundaries were fixed. On the other hand, in the dynamic analyses viscous absorbent boundaries were used on the sides to avoid reflections. Acceleration time histories were prescribed on the bottom boundary.

Table 2. FS and inclinations at different heights

H (m)	*i* (°)	*FS*
Clay-1		
5	30°	1.02
10	20°	1.01
15	17°	1.02
Clay-2		
5	40°	1.05
10	25°	1.03
15	22°	1.04
Sand		
5	35°	1.03
10	32°	1.03
15	30°	1.06

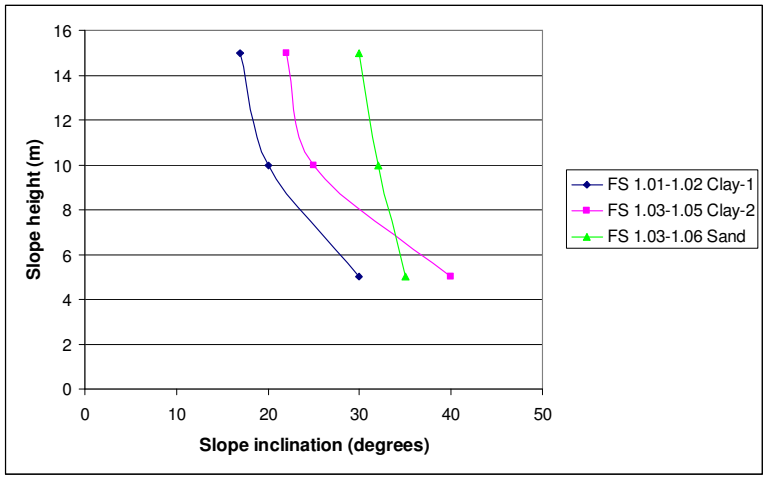

Figure 3. Critical slope angles for each height

Soil properties and behaviour

The physical and mechanical properties of the sand and the clay-1 are summarized in Table 3. This table shows the variations used in stiffness for the sand and clay slopes, and the strength variation for the two clays. As the variation with depth of the stiffness and strength could not be incorporated exactly due to the topography, a re-adaptation was taken into account to represent the soil parameter variations through the subunits or regions displayed in Figure 4.

Clay slopes

To account for the increase in stiffness and strength of the soil with depth, the slopes were modelled with thin layers or subunits of constant properties in each layer (Figure 4a). The stiffness variation with depth was estimated according to empirical equations, Equation 1 for the upper two subunits and Equation 2 for the remaining subunits:

$$G_{\max} = 700 c_u \qquad (1)$$

$$G_{\max} = 850 c_u \qquad (2)$$

Table 3. Geotechnical parameters of the modelled soils

Parameter	**Name**	**Sand**	**Clay-1**	**Unit**
Material model	*Model*	Mohr Coulomb	Mohr Coulomb	-
Material behaviour	*Type*	Drained	Drained	-
Soil unit weight	γ	18.0	18.6	kN/m^3
Young's modulus at reference level y_{ref}	E_{ref}	2.814e+5	9720	kPa
E gradient of *E* with depth	E_{incr}	1.236E+4	-	kPa/m
Reference level	y_{ref}	-5	-	m
Poisson's ratio	ν	0.35	0.33	-
Shear wave velocity	v_s	238	44	m/s
Cohesion	c_{ref}	0.5	6.8	kPa
Friction angle	φ	30	0	°
Dilatancy angle	ψ	0	0	°
Rayleigh damping constants:	α β	0.23 0.003	0.23 0.003	- -

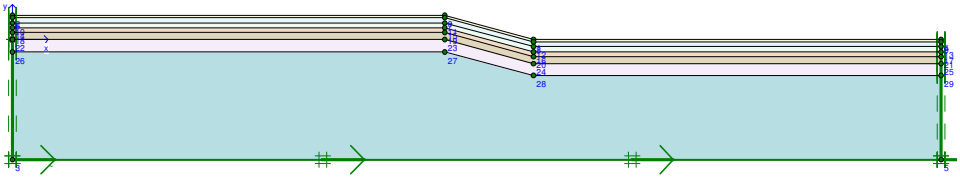

(a) Clay slope geometry, 10 m height (*H*), 15° steep (*i*)

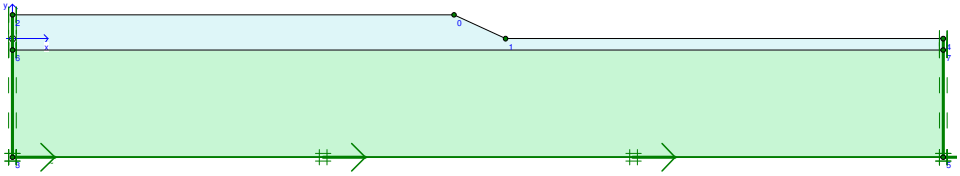

(b) Sand slope geometry, 10 m height (*H*), 25° steep (*i*)

Figure 4. Slope geometries: (a) Clay, (b) Sand

The shear strength as a function of stress was calculated according to Equation 3, for "clay 1" at the upper and second layers or subunits, and Equation 4 for the lower regions of the same clay. The value of the upper subunit was taken at its base (1 m depth). The strength for the second and subsequent layers was estimated at their middle point (e.g. 2 m depth for Layer 2).

$$c_u = 0.28\sigma_v' \tag{3}$$

$$c_u = 0.25\sigma_v' \tag{4}$$

The second clay ("clay 2") had the same stiffness but higher strength. The strength increment was implemented as given in Equation 5 for the upper two subunits and Equation 6 for the remaining ones. The depths were assigned in the same way as for the "clay 1".

$$c_u = 0.33\sigma_v' \tag{5}$$

$$c_u = 0.30\sigma_v' \tag{6}$$

Sand slopes

For the sand, only two sub-regions were used. The upper region ("*upper subunit*") was considered homogenous. The lower region (below a depth of -5 m. Figure 4b) was modelled with variable stiffness. G_{max} was estimated from the following relation (Hardin & Richart, 1963):

$$G_{\max} = 3300\frac{(2.973-e)^2}{1+e}\sigma_0'^{1/2} \tag{7}$$

where: e= void ratio, assumed equal to 0.5; and σ_0' = mean principal effective stress

Constitutive model and damping

The Mohr Coulomb material behaviour was used for simplicity and to allow the development of permanent strains. The damping of the system was Rayleigh type. In time-domain analyses the Rayleigh damping gives an approximation of frequency independent damping over a narrow frequency band. The selected band was between 0.4 and 5 Hz. The resultant mass (α) and stiffness (β) proportional constants (Table 3) were estimated for a 5% damping from:

$$\alpha + \beta\omega_i^2 = 2\omega_i\xi_i \tag{8}$$

Dynamic loads

The dynamic loads were sinusoidal functions, expressed as acceleration time histories, with frequencies of 1, 2 and 4 Hz and amplitude variations as displayed in Figure 2. These accelerations were increased gradually between 0.01 g and 0.32 g for the clay slopes and 0.15 g to 1.0 g for the sand slopes until failure was reached. The slope was assumed to fail when the Cartesian shear strains (γ_{xy}) were in the range of 10 to 15%. The peak critical acceleration (*PGAc*) for each frequency necessary to trigger the failure was then established. All the acceleration time histories had durations of 20 s (Figure 2) and were monochromatic for simplicity and for isolating the effects of the input frequency and amplification of the waves through the slope.

Natural period of site

From the model properties, the natural periods and frequencies of oscillation of the soils were calculated using Equation 9, in which *Vs* is the average the shear wave velocity (*Vs*) of the soil (Table 4). This was estimated for the region behind the slope crest (assumed as free field):

$$T = \frac{4H}{Vs} \tag{9}$$

Table 4. Averaged *Vs*, natural periods and frequencies of the models

Soil unit	*H*	Vs_{av} (m/s)	*Tn* (s)	*fn* (Hz)
Clay	5	161.3	1.36	0.74
	10	162.2	1.48	0.68
	15	163.5	1.59	0.63
Clay-2	10	162.2	1.48	0.68
Sand	10	238.2	1	1

CRITICAL ACCELERATIONS TO TRIGGER SLOPE INSTABILITIES

Several slope geometries were considered in the analyses. By increasing the input acceleration until the shear strain distribution suggested slope instability (e.g. Figure 5), the maximum horizontal acceleration or critical acceleration (*PGAc*) was obtained. The slip surfaces in the clay models were located at about 3 m below the slope face. The sand displayed less continuous slip surfaces (Figure 5b).

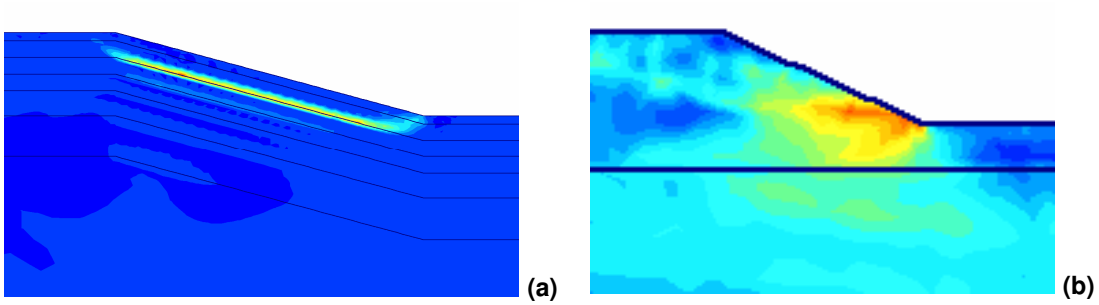

Figure 5. Cartesian shear strains (γ_{xy}) at failure moment for (a) clay (γ_{xy}=12%, *H*=10 m, *i*=15°, *f*=2 Hz) and (b) sand (γ_{xy}= 10%, *H*=10 m, *i*=25°, *f*=2 Hz)

Various trends were found between the *PGAc* and the slope parameters (*H*, *i*) and input frequencies of the signals. The graphical results for each material are shown in Figure 6 and summarized as the following:

- Clay 1: *PGAc* at *f*=4 Hz > *PGAc* at *f*=2 Hz > *PGAc* at *f*=1 Hz

- Clay 2: *PGAc* at f=4 Hz > *PGAc* at f=2 Hz. And:
    - *PGAc* at f=2 Hz > *PGAc* at f=1 Hz if $i \geq 15°$, when H=10 m
    - *PGAc* at f=2 Hz > *PGAc* at f=1 Hz if $i > 20°$, when H=15 m
    - *PGAc* at f=1 Hz > *PGAc* at f=4 Hz if $i < 15°$, when H=15 m
- Sand:
    - *PGAc* at f=4 Hz > *PGAc* at f=2 Hz and 1 Hz if $i \geq 20°$, when H=10 m
    - *PGAc* at f=4 Hz > *PGAc* at f=2 Hz and 1 Hz if $i \geq 20°$, when H=15 m
    - *PGAc* at f=2 Hz > *PGAc* at f=1 Hz if $i < 25°$, when H=15 m

At the lower inclinations the slip surface was not well developed and the spatial distribution of the shear strains was not entirely clear. The following are these cases:

- Clay 1: $i \leq 10°$, when H=15 m and f=1 Hz, $i \leq 5°$, when H=15 m and f=2 Hz
- Clay 2: $i \leq 10°$, when H=10 and 15 m and f=1 Hz
- Sand: $i \leq 25°$, when H=5 m and f=1 and 4 Hz
  $i \leq 20°$, when H=5 and 15 m and f=2 Hz
  $i \leq 15°$, when H=15 m and f=1 and 4 Hz

As expected, the values of *PGAc* decrease at steeper slopes and weaker materials. The "clay 1" presents critical accelerations from 0.01 g to 0.25 g, slightly lower than for the stronger "clay 2", of which the *PGAc*s range between 0.02 g and 0.32 g (Figure 6 and Figure 7). The sand needs stronger accelerations to develop slope instabilities (0.15 g to 1.0 g, as seen in Figure 6). The sand displays a steeper trend in the curves of *PGAc* values (Figure 7) due to its higher strength.

In general, in the clays the higher frequencies require larger *PGAc* in order to lead to slope instabilities with a few exceptions for the higher slopes (Figure 6, Figure 7 and Figure 8). For the sand that applies only for the highest frequency considered (f=4 Hz). In this material, the other frequencies do not show any clear pattern when H=10 m, but for H=5 m and H=15 m the 2 Hz records have higher *PGAc* than the 1 Hz ones when the slopes are H=5 and i<30° m and H=15 m and i<25°.

Considering the *PGAc* tendencies for each soil type (Figure 8) it can be concluded that lower heights need higher *PGA* values in order to develop instabilities in the slopes. The main findings are:

- Clay 1: *PGAc* at H=5 m > *PGAc* at H=10 m > *PGAc* at H=15 m
- Clay 2: *PGAc* at H=5 m > *PGAc* at H=10 m > *PGAc* at H=15 m
- Sand: *PGAc* at H=5 m > *PGAc* at H=10 m and at H=15 m. In this material, the *PGAc*s of the 15 m height slopes have a broader range than that of H=10 m.

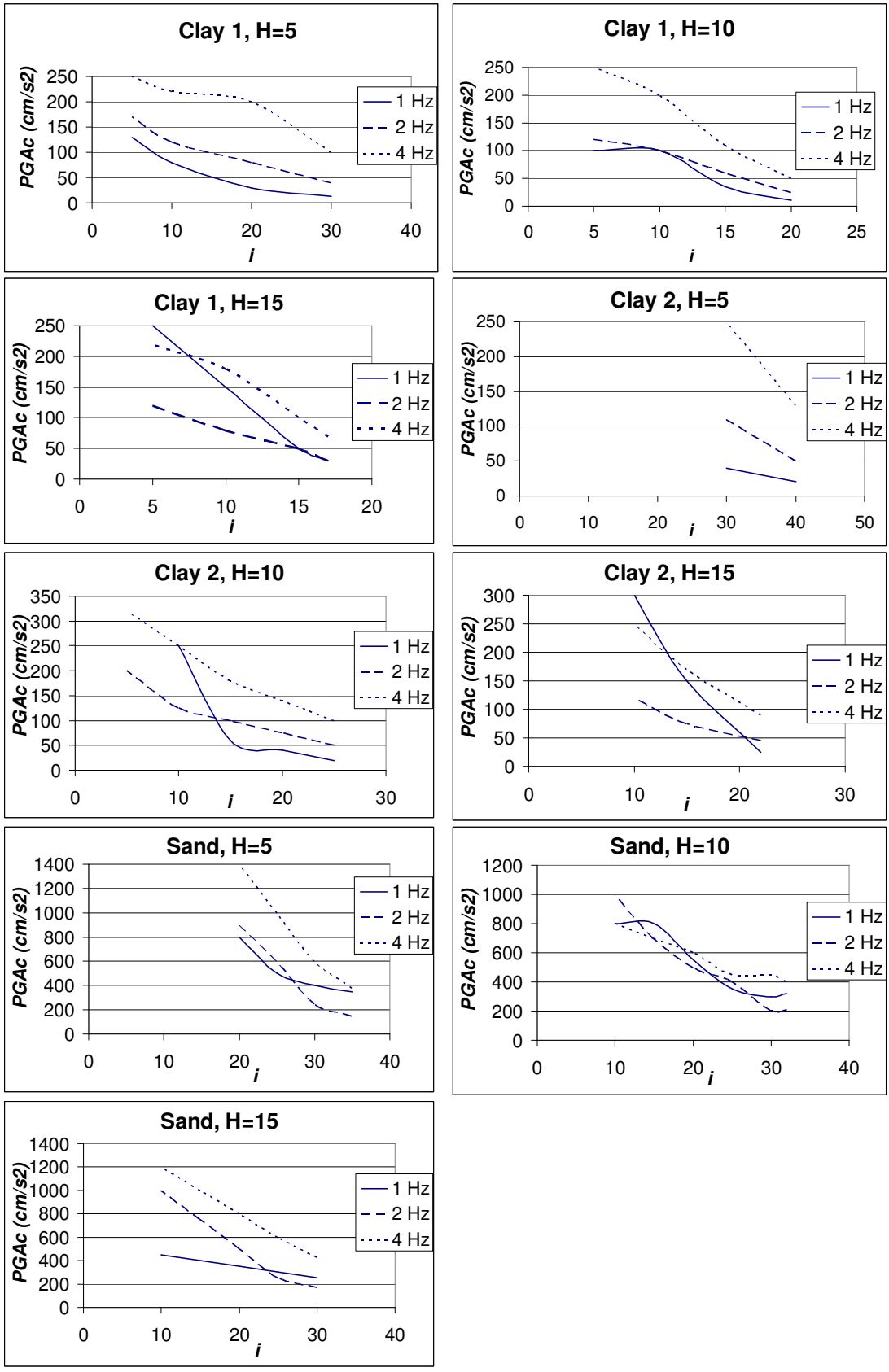

Figure 6. Critical accelerations per soil type and slope height

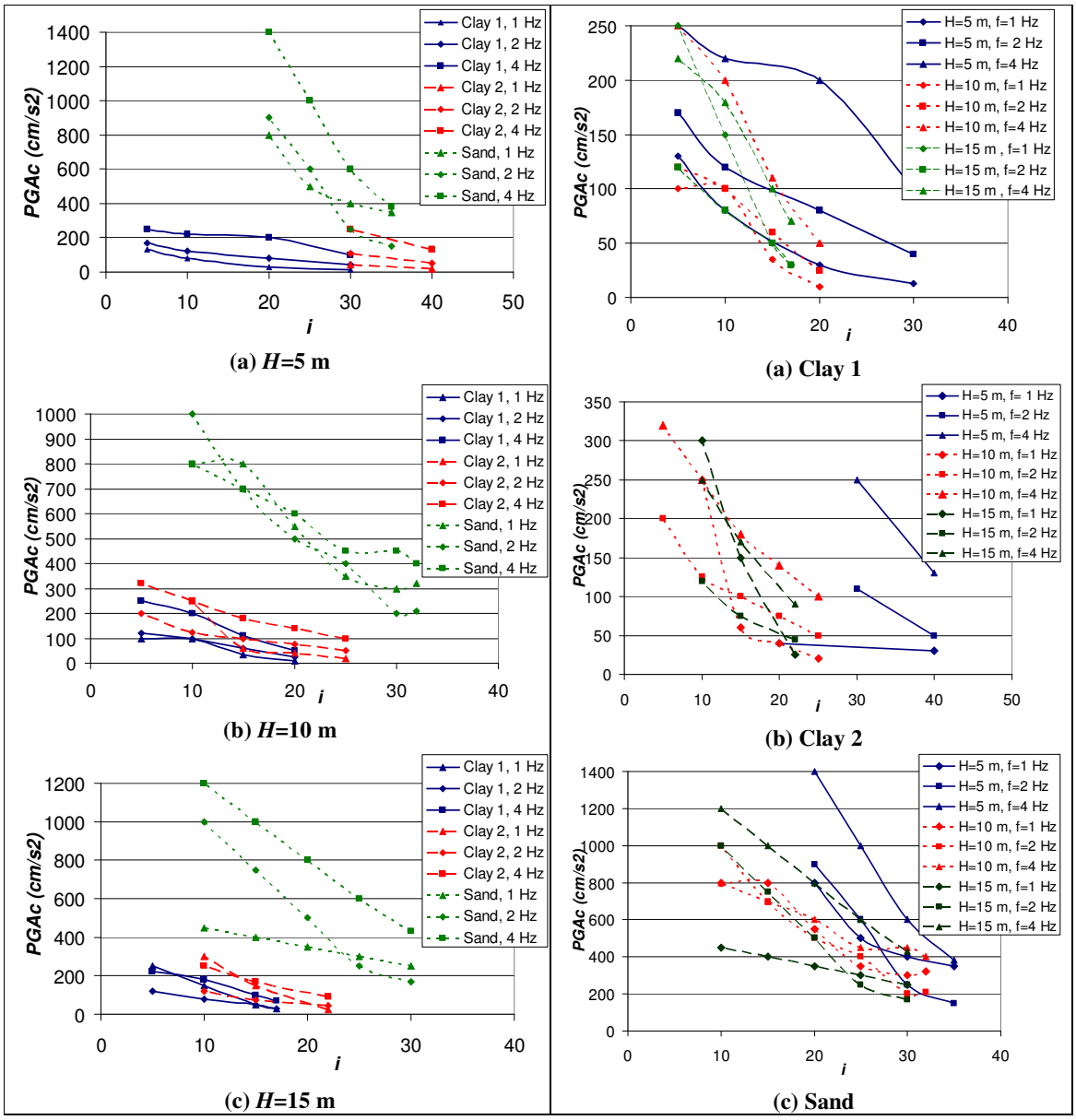

Figure 7. Critical accelerations variation with the slope inclination at *H*=5 m (a), *H*=10 m (b) and *H*=15 m (c)

Figure 8. Critical accelerations variation with the slope inclination for clay-1 (a), clay-2 (b) and sand (c)

PRACTICAL CONSIDERATIONS

The analyses presented in this study have been performed with ideal and simplified soil, slope and input accelerations conditions. However, real slopes represent more variable soil parameters and have more complicated geometries. Analyses of real slopes may take enormous computational time which may not justify their use. The acceleration time histories used in this study were monochromatic. The objective has been to use a simple excitation in order to isolate the effect of the input frequency and amplification of the seismic waves through the slope. This may bias the results and observations. Nevertheless, it is believed that the above results provide useful insight into the important parameters and the need for more involved computations for real cases.

CONCLUSIONS

The numerical results of this parametric study provide estimates of earthquake thresholds for slope instabilities. These results are applicable to the specified generic soil types (clays and sand) under dry conditions in two dimensional plane strain space. The results provide insight into the impact of the various parameters on the seismic stability of slopes. Some trends were obtained for the critical accelerations triggering slides at different geometries for the selected cases. The sand displays higher thresholds than the clays (0.15 g to 1.0 g compared to 0.01 g to 0.32 g). The clay with lower strength ("clay 1") had lower *PGAc* values (0.01 g to 0.25 g) than the clay with higher strength ("clay 2": 0.02 g to 0.32 g), as shown in Figure 7 and Figure 8. Consistently, all the *PGAc* values decrease with slope inclination increments.

Lower heights need higher *PGAc* in order to trigger slides as logically expected. But this is not clear for the higher slopes in the sand (H=10 m and H=15 m) because their *PGAc* values fall within similar ranges (Figure 8).

In terms of frequency, the higher frequency assessed (4 Hz) always showed higher slope instability thresholds, consistently in all the soils analysed. In the clays, the PGAc values tend to decrease for lower frequencies, with a few exceptions for the less steep slopes. Some of the sand slopes also show that trend, although this observation is less clear for this material.

The 1 Hz loads are closer to the natural frequencies of site. Therefore, the lower slope failure thresholds obtained at that frequency can be related to a site effect or resonance that can even have developed local amplification and/or tension induced by surficial waves reflected at the surface.

The nonlinearity is only partially achieved as the shear moduli and shear strength vary in depth, but the damping condition is frequency dependent (Rayleigh) and no reduction in the stiffness was incorporated at this stage of the investigation. Further research is planned to consider the effect of stiffness reduction and hysteretic damping as well as softening material models. Moreover, it is planned to simulate the results of experimental studies and case histories. Realistic earthquake excitation will be used in future analyses.

AKNOWLEDGEMENTS

This work is being sponsored by the Strengthening Local Authorities in Risk Management (SLARIM) project of ITC, The Netherlands, with additional support from the International Centre of Geohazards (ICG) & the Norwegian Geotechnical Institute (NGI), Norway. The first author would like to express her special gratitude to Dr. R. Brinkgreve for his support related to use of PLAXIS.

REFERENCES

Ashford, S.A. and Sitar, N. "Simplified method for evaluating seismic stability of steep slopes," Journal of Geotechnical Geoenvironmental Engineering, ASCE, 128, 119-128, 2002.

Azizian, A. and Popescu, R. "Three-dimensional seismic analysis of submarine slopes," Soil Dynamics and Earthquake Engineering, 26, 870-887, 2006.

Bird, J.F. and Bommer, J.J. "Earthquake losses due to ground failure," Engineering Geology, 75, 147-179, 2004.

Bommer, J.J. and Rodríguez, C.E. "Earthquake-induced landslides in Central America," Engineering Geology, 63, 189-220, 2002.

Bourdeau, C., Havenith, H.-B., Fleurisson, J.-A., and Grandjean, G. "Numerical Modelling of Seismic Slope Stability," Springer Berlin, in Engineering Geology for Infrastructure Planning in Europe, H.R.G.K. Hack, R. Azzam, R. Charlier (Eds.), Volume 104/2004, 671-684, 2004.

Chang, K.-J., Taboada, A., Lin, M.-L., and Chen, R.-F. "Analysis of landsliding by earthquake shaking using a block-on-slope thermo-mechanical model: Example of Jiufengershan landslide, central Taiwan," Engineering Geology, 80, 151-163, 2005.

Chugh, A.K. and Stark, T.D. "Permanent seismic deformation analysis of a landslide," Landslides, 3, 2-12, 2006.

Crosta, G.B., Imposimato, S., Roddeman, D., Chiesa, S., and Moia, F. "Small fast-moving flow-like landslides in volcanic deposits: The 2001 Las Colinas Landslide (El Salvador)," Engineering Geology, 79, 185-214, 2005.

Esposito, E., Porfido, S., Simonelli, A.L., Mastrolorenzo, G., and Iaccarino, G. "Landslides and other surface effects induced by the 1997 Umbria-Marche Seismic Sequence," Engineering Geology, 58, 353-376, 2000.

Fukuoka, H., Wang, G., Sassa, K., Wang, F., and Matsumoto, T. "Earthquake-induced rapid long-traveling flow phenomenon: May 2003 Tsukidate landslide in Japan," Landslides, 2, Issue 2, 151-155, 2004.

Ghosh, B. and Madabhushi, S.P.G. "A numerical investigation into effects of single and multiple frequency earthquake motions," Soil Dynamics and Earthquake Engineering, 23, 691-704, 2003.

Havenith, H.-B., Jongmans, D., Faccioli, E., Abdrakhmatov, K., and Bard, P.-Y. "Site effect analysis around the seismically induced Ananevo Rockslide, Kyrgyzstan," Bulletin of the Seismological Society of America, 92, Issue 8, 3190-3209, 2002.

Havenith, H.-B., Vanini, M., Jongmans, D., and Faccioli, E. "Initiation of earthquake-induced slope failure: influence of topographical and other site specific amplification effects," Journal of Seismology, 7, Issue 3, 397-412(16), 2003.

Hardin, B.O. and Richart, F.E. "Elastic wave velocities in granular soils," Journal of Soil Mechanics and Foundations, ASCE, 89, SM1, 33-65, 1963.

Kagawa, T., Sato, M., Minowa, C., Abe, A., and Tazoh, T. "Centrifuge simulations of large-scale shaking table tests: case studies," Journal of Geotechnical and Geoenvironmental Engineering, 130, Issue 7, 663-672, 2004.

Keefer, D.K. "Landslides caused by earthquakes," Geological Society of America Bulletin, 95, 406-421, 1984.

Keefer, D.K. "The Loma Prieta, California earthquake of October 17, 1989 – Landslides," US Geol. Survery, Profesional Paper 1551-C, 183 pp., 1998.

Keefer, D.K. "Statistical analysis of an earthquake-induced landslide distribution – The 1989 Loma Prieta, California event," Engineering Geology, 58, 231-249, 2000.

Keefer, D.K. "Investigating landslides caused by earthquakes – A historical review," Surveys in Geophysics, 23, 473-510, 2002.

Khazai, B. and Sitar, N. "Evaluation of factors controlling earthquake-induced landslides caused by Chi-Chi earthquake and comparison with the Northridge and Loma Prieta events," Engineering Geology, 71, 79-95, 2003.

Kokusho, T. and Ishizawa, T. "Energy approach for earthquake induced slope failure evaluation," Soil Dynamics and Earthquake Engineering, 26, 221-230, 2006.

Kramer, S.L. and Stewart, J.P "Geotechnical Aspects of Seismic Hazards," In: Earthquake Engineering: from Engineering Seismology to Performance-Based Engineering, Y. Bozorgnia, V. Bertero (Eds.), CRC Press, Chapter 4, 85 pp., 2004.

Leroueil, S. "Natural slopes and cuts: movement and failure mechanisms," Géotechnique, 51, Issue 3, 197-243, 2001.

Loukidis, D., Bandini, P., and Salgado, R. "Stability of seismically loaded slopes using limit analysis," Géotechnique, 53, Issue 5, 463-479, 2003.

Lu, J. "Parallel finite element modeling of earthquake ground response and liquefaction," PhD dissertation, University of California, San Diego, 359 pp., 2006.

Nabeshimal, Y., Tokida, K., Nakahira, A., Ohtsuki, A., and Nakayama, Y. "Dynamic centrifuge model test of road Embankment," Proceedings on the 2nd Japan-Taiwan Joint Workshop,

Geotechnical Hazards from Large Earthquakes and Heavy Rainfall, Nagaoka, Niigata, Japan, ATC3 (Geotechnology for Natural Hazards), May 18-20, 177-182, 2006.

Ng, C.W.W., Li, X.S., van Laak, P.A., and Hou, D.Y.J. "Centrifuge modeling of loose fill embankment subjected to uni-axial and bi-axial earthquakes," Soil Dynamics and Earthquake Engineering, 24, 305-318, 2004.

Nicoletti, P.G. and Parise, M. "Seven landslide dams of old seismic origin in south-eastern Italy," Geomorphology, 46, 203-222, 2002.

Papadopoulos, G.A. and Plessa, A. "Magnitude-distance relations for earthquake-induced landslides in Greece," Engineering Geology, 58, 377-386, 2000.

Popescu, R. and Prevost, J.H. "Centrifuge validation of a numerical model for dynamic soil liquefaction," Soil Dynamics and Geotechnical Earthquake Engineering, 12, 73-90, 1993.

Porfido, S., Esposito, E., Vittori, E., Tranfaglia, G., Michetti, A.M., Blumetti, M., Ferreli, L., Guerrieri, L., and Serva, L. "Areal distribution of ground effects induced by strong earthquakes in the southern Apennines (Italy)," Surveys in Geophysics, 23, 529-562, 2002.

Prestininzi, A. and Romeo, R. "Earthquake-induced ground failures in Italy," Engineering Geology, 58, 387-397, 2000.

Rodríguez, C.E., Bommer, J.J., and Chandler, R.J. "Earthquake-induced landslides: 1980-1997," Soil Dynamics and Earthquake Engineering, 18, 325-246, 1999.

Sassa, K., Fukuoka, H., Wang, G., and Ishikawa, N. "Undrained dynamic-loading ring-shear apparatus and its application to landslide dynamics," Landslides, 1, Issue 1, 7-19, 2004.

Sepúlveda, S.A., Murphy, W, and Petley, D.N. "Topographic controls on coseismic rock slides during the 1999 Chi-Chi earthquake, Taiwan," Quaterly Journal of Engineering Geology and Hydrogeology, 38, 189-196, 2005.

Taboada-Urtuzuastegui, V.M., Martinez-Ramirez, G., and Abdoun, T. "Centrifuge modeling of seismic behavior of a slope in liquefiable soil" Soil Dynamics and Earthquake Engineering, 22, 1043-1049, 2002.

Tibaldi, A., Ferrari, L., and Pasquare, G. "Landslides triggered by earthquakes and their relations with faults and mountain slope geometry: an example from Ecuador," Geomorphology, 11, 215-226, 1995.

Trandafir, A.C. and Sassa, K., "Seismic triggering of catastrophic failures on shear surfaces in saturated cohesionless soils," Canadian Geotechnical Journal, 32, 229-251, 2005.

Uzuoka, R., Sento, N., Kazama, M., and Unno, T. "Landslides during the earthquakes on May 26 and July 26, 2003 in Miyagi, Japan," Soils and Foundations, 45, Issue 4, 149-163, 2005.

Wartman, J., Bray, J.D., and Seed, R.B., "Inclined plane studies of the Newmark sliding block procedure," Journal of Geotechnical and Geoenvironmental Engineering,129, Issue 8, 673-684, 2003.

Wasowski, J., del Gaudio, V., Pierri, P., and Capolongo, D. "Factors controlling seismic susceptibility of the Sele valley slopes: the case of the 1980 Irpinia earthquake re-examined," Surveys in Geophysics, 23, 563-593, 2002.

Wen, B., Wang, S., Wang, E., and Zhang, J. "Characteristics of rapid giant landslides in China," Landslides, 1, Issue 4, 247-261, 2004.

Wright, S.G. and Rathje, E.M. "Triggering mechanisms of slope instability and their relationship to earthquakes and tsunamis," Pure and Applied Geophysics, 160, 1865-1877, 2003.

Zeghal, M., Elgamal, A.-W., Zeng, X., and Arulmoli, K. "Mechanism of liquefaction response in sand-silt dynamic centrifuge tests," Soil Dynamics and Earthquake Engineering, 18, 71-85, 1999.

Zergoun, M. and Vaid, Y.P. "Effective stress response of clay to undrained cyclic loading," Canadian Geotechnical Journal, 31, 714-727, 1994.